

Microfluidic Generation of Monodisperse, Structurally Homogeneous Alginate Microgels for Cell Encapsulation and 3D Cell Culture

Stefanie Utech, Radivoje Prodanovic, Angelo S. Mao, Raluca Ostafe, David J. Mooney, and David A. Weitz*

Micrometer-sized alginate particles are used for the encapsulation of living cells in pharmaceutical research, tissue engineering, and regenerative medicine.^[1–5] Such microgels act as micrometer-sized 3D culturing units allowing individual cells to be independently monitored or manipulated for example to study the role confinement on cell fate or to deliver cells for the repair of damaged tissue.^[6,7] The ideal microgel particles for these applications should be composed of a homogenous network structure allowing the stable entrapment of the encapsulated cell in a controlled microenvironment with precise internal structure. Additionally, particle sizes should be small (<200 μm) to enable effective delivery of oxygen and nutrients to the encapsulated cell which is essential for cell viability and health.^[8–10] In tissue engineering, cell-containing microgels are also used as building blocks that are assembled into larger architectures mimicking the structure of tissues and organs.^[7,11] Since cell–cell distances and structural arrangement have significant influence on cellular properties and function, a precise control over size and size distribution is of key importance.^[12]

Alginate microgel particles can be produced by means of droplet-based microfluidics which combines high-throughput production with precise control over size, shape, and morphology of the generated droplets.^[3,9,13–15] Typically, an aqueous

alginate solution is emulsified in an oil phase and crosslinked ionically with bivalent ions such as Ca^{2+} . The ionic crosslinking process occurs immediately upon contact of alginate chains and calcium ions. The fast reaction typically results in uncontrolled gelation within the microfluidic device that can cause clogging and nonuniform drop formation.^[8,16] To overcome these problems, the drop formation and the gelation reaction must be separated. Thus, calcium ions need to be delivered to the alginate solution without inducing unintended gelation prior to drop formation.

One route to achieve this goal is the use of calcium carbonate (CaCO_3) nanoparticles.^[2,13,17] The water-insoluble particles are dispersed in the alginate solution and can be dissolved under acidic conditions after drop formation. Premature gelation is avoided and monodisperse particles result. However, the dissolution of solid calcium salt particles causes a heterogeneous distribution of calcium ions inside the droplets and diminishes the homogeneity of the resulting particles. Additionally, clogging of small microfluidic channels in the presence of particle aggregates limits the range of accessible microgel dimensions.^[13] Other techniques involve the initiation of the crosslinking process by the delivery of calcium chlorides or acetate particles through the oil phase which are subsequently dissolved in the emulsion droplet.^[17,18] Nevertheless, this method can suffer from the same problems, namely inhomogeneous calcium distribution or clogging issues. Alternatively, the generation of alginate microgels via coalescence of separate droplets containing alginate and calcium chloride has been tried.^[19] However, mixing inside the coalesced droplets still results in heterogeneous particles since crosslinking takes place before a homogenous distribution of calcium ions can be achieved. Additionally, coalescence generally results in a volume increase of the final, crosslinked alginate microgels.^[17]

If we were able to control the crosslinking process, homogenous microgel particles with reliable and precisely tunable particle properties would become accessible. This would allow us to study the influence of the physical properties of the microgel matrix on the behavior of the encapsulated cell in three dimensions which is of great importance for applications in tissue engineering, stem cell research, and the treatment of diseases.^[20–22] However, the limited homogeneity of available alginate microgels particles restricts these applications.

In this communication, we present a method for the fabrication of monodisperse alginate microgels with structural homogeneity via droplet-based microfluidics. We deliver calcium ions in the form of a water-soluble calcium–ethylenediaminetetraacetic

Dr. S. Utech, Prof. R. Prodanovic, A. S. Mao,
Dr. R. Ostafe, Prof. D. J. Mooney, Prof. D. A. Weitz
School of Engineering and Applied Sciences
Harvard University
02138 Cambridge, MA, USA
E-mail: weitz@seas.harvard.edu

Prof. R. Prodanovic
Faculty of Chemistry
University of Belgrade
Studentski trg 12, 11000 Belgrade, Serbia

Dr. R. Ostafe
Molecular Biotechnology
Faculty of Biology
RWTH Aachen University
52062 Aachen, Germany

Prof. D. J. Mooney
Wyss Institute for Biologically Inspired Engineering
02138 Cambridge, MA, USA

Prof. D. A. Weitz
Department of Physics
Harvard University
02138 Cambridge, MA, USA



DOI: 10.1002/adhm.201500021

acid (calcium–EDTA) complex. By chelating the calcium ions with EDTA, the ions remain in solution but are inaccessible to the alginate chains. Using droplet-based microfluidics, we emulsify a perfectly homogenous mixture of alginate and the chelated calcium ions without inducing unintended gelation. By addition of acetic acid to the continuous phase, we trigger the dissociation of the complex and release calcium ions after drop formation. The free ions react with the alginate chains in a highly controlled fashion forming alginate microgels with excellent structural homogeneity. By separating drop formation and crosslinking in this purely aqueous system, we eliminate clogging issues and generate alginate microgel particles with particle size down to 10 μm and narrow particle size distributions. We demonstrate that the gelation process is suitable for the encapsulation of living cells by encapsulating individual mesenchymal stem cells (MSCs). Our mild polymerization technique allows us to encapsulate the cells with high viability. We culture and monitor the encapsulated cells inside the microgels over the course of two weeks within which we observe stable encapsulation, healthy cells, growth, and proliferation.

We prepare monodisperse, structurally homogeneous alginate microgels in the size range of 10–50 μm by acidic dissociation of a water-soluble calcium–EDTA complex within an alginate containing emulsion droplet. We form the calcium–EDTA

complex by mixing a solution of calcium chloride ($100 \times 10^{-3} \text{ M}$) with a solution of disodium–EDTA ($100 \times 10^{-3} \text{ M}$) in equal ratios, schematically illustrated in **Figure 1a**. We adjust the pH value of the solution using sodium hydroxide until we reach a pH of 7. Under neutral conditions the complex is highly stable. The chelation of calcium ions with EDTA keeps the ions in solution but impedes their reaction with alginate chains. We are thus able to prepare a homogenous mixture of the aqueous calcium–EDTA complex solution ($50 \times 10^{-3} \text{ M}$) and an aqueous alginate solution (2 wt% MVG, Novamatrix). We use a FITC-labeled alginate, prepared using carbodiimide chemistry, which enables visualization of the internal structure of the microgel after polymerization using fluorescence microscopy.^[7] The premixed alginate–calcium–EDTA complex solution is emulsified into monodisperse droplets using a microfluidic flow-focusing device as shown in **Figure 1b,c**. Fluorinated carbon oil (HFE7500, 3 M) containing 1 wt% of a biocompatible surfactant is used as the continuous phase.^[23] After drop formation, gelation is induced by the addition of acetic acid (0.05 vol%) to the oil phase. The acid diffuses into the droplets and causes a decrease in pH, leading to the dissociation of the Ca–EDTA complex and the release of calcium ions. The liberated calcium ions then react with the alginate chains creating uniformly crosslinked microgel particles, illustrated in **Figure 1d**. After

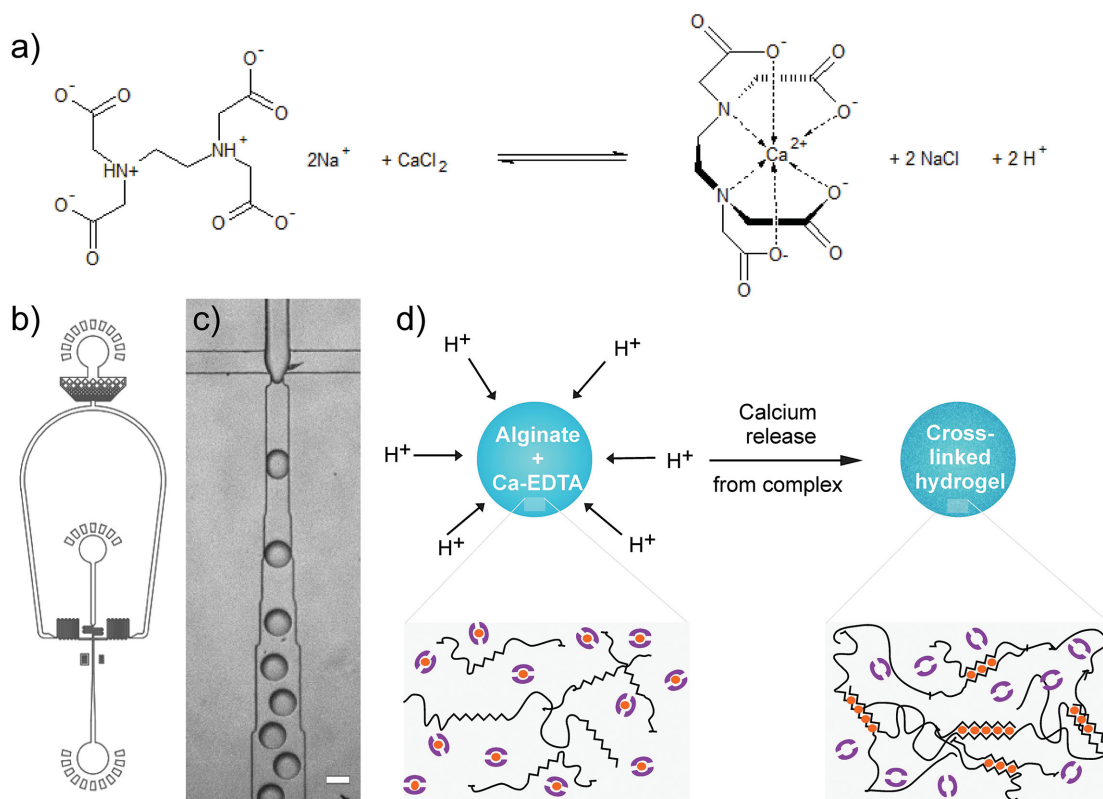


Figure 1. Microfluidic generation of homogeneously crosslinked alginate microparticles by on-demand release of calcium ions from a water-soluble calcium–EDTA complex. a) Reaction scheme for the formation and dissociation of the calcium–EDTA complex. Under neutral conditions (pH 7.0) the calcium ions are chelated by the EDTA molecules. In an acidic environment (pH 5.0), the reverse reaction takes place resulting in a release of calcium ions that can then form an ionic network with the alginate chains. b,c) Schematic illustration (b) and microscopic image (c) of the microfluidic flow-focusing device used for the fabrication of alginate microbeads (scale bar: 50 μm). d) Schematic illustration of the crosslinking process. Upon addition of acid to the continuous phase, the calcium–EDTA complex dissolves, calcium ions are released, and crosslinking of alginate is induced.

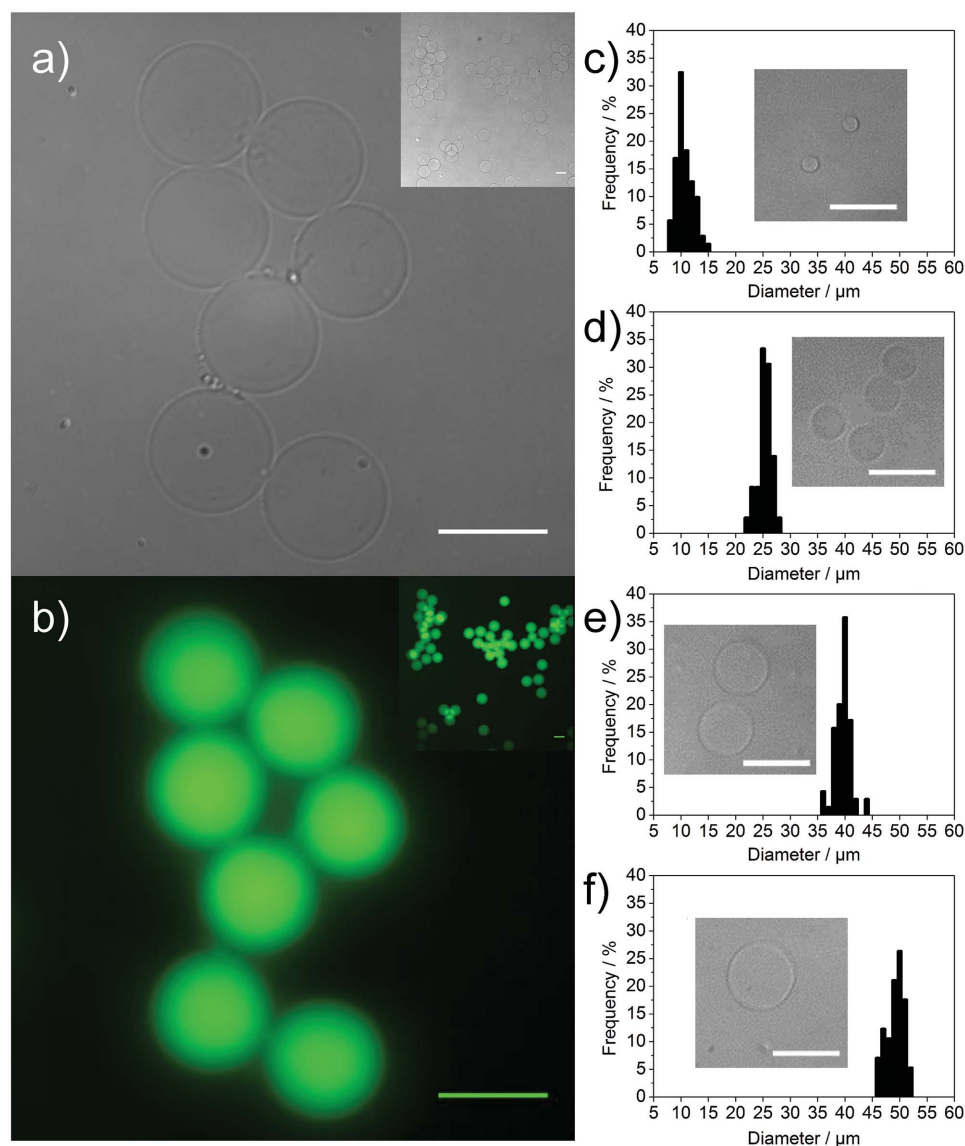


Figure 2. a,b) Bright-field and fluorescent images of alginate microbeads after transfer into aqueous medium. The images reflect the high monodispersity of the spherical particles. The high-magnification fluorescent image reveals the homogeneous structure of the alginate microbeads. c–f) Representative bright-field images and corresponding size distribution histograms of homogeneous alginate microbeads with 10, 25, 40, and 50 μm in diameter. The gels are prepared using three different microfluidic devices (10, 25, and 50 μm channels). The flow rate of the inner phase (alginate–calcium–EDTA) solution is 50 $\mu\text{L h}^{-1}$. The flow rate of the continuous oil phase is varied between 100 and 500 $\mu\text{L h}^{-1}$ to adjust the size of the droplets for a given microfluidic device. By separating the gelation from the drop formation process and the use of merely water-soluble materials, a precise control of the drop formation and hence, particle size and size distribution is achieved. All scale bars are 50 μm .

gelation, the microgels are transferred into aqueous medium. The water-soluble nature of the complex eliminates clogging issues arising in case of solid crosslinking precursors and allows the homogenous distribution of calcium ions inside the aqueous droplet prior to gelation.^[2,13,17] We avoid premature gelation by the time-controlled dissociation of the complex which furthermore allows the separation of drop formation and crosslinking process resulting in a highly controlled and consequently, reliable and reproducible drop and subsequent particle generation. Bright-field images of the microgels, taken after transfer to an aqueous medium reveal the high monodispersity of the particles as shown in **Figure 2a**. Fluorescence

microscopy images illustrate the internal morphology of the microgel particles. The fluorescence intensity and consequently the concentration of alginate are homogenous throughout the particle confirming the expected structural homogeneity, visible in **Figure 2b**. A comparison between different preparation methods of microfluidically generated alginate microgels nicely demonstrates the superior homogeneity of the presented particles as shown in **Figure S1** (Supporting Information).

Alginate microgels can also be prepared by using higher concentration of the calcium–EDTA complex (data not shown). However, the limited solubility of EDTA in water which is around 0.26 M at 20 °C can cause the formation of insoluble

precipitates which impedes the aspired structural homogeneity. The same problem occurs for calcium–EDTA concentrations higher than $100 \times 10^{-3} \text{ M}$ when mixed with 2 wt% alginate. The concentration of calcium–EDTA can also be lower than the ones applied here. However, the critical calcium concentration necessary to ensure complete gelation of alginate has been reported to be in the order of $25 \times 10^{-3} \text{ M}$.^[24] The relation between calcium–EDTA concentration and drop formation efficiency is illustrated in Figure S2 (Supporting Information). A 2 wt% alginate concentration is the highest concentration that can be used under the presented conditions. The high viscosity of alginate solutions with concentrations higher than 2 wt% results in debonding of the microfluidic device due to the high pressures generated inside the microchannels, especially in case of small dropmakers.

The size of the alginate microgels can be adjusted by changing the size of the microfluidic device and the applied flow rates. We use three flow-focusing devices with different

square cross-sectional dimensions. We keep the flow rate of the alginate–calcium–EDTA solution constant ($50 \mu\text{L h}^{-1}$), while varying the flow rate of the continuous phase from 100 to $500 \mu\text{L h}^{-1}$, thereby decreasing the drop size for a given drop-maker (see Supporting Information). We prepare particles as small as $10 \mu\text{m}$ using a microfluidic device with a $10 \mu\text{m}$ square cross-sectional channel. Larger gel sizes are made with larger microfluidic channels as shown for 25, 40, and $50 \mu\text{m}$ particles. All samples exhibit narrow size distributions and excellent homogeneity, illustrated in Figure 2c–f.

We demonstrate the suitability of the method presented for 3D cell culture application by encapsulating living mesenchymal stem cells (MSCs) into microgels. We choose a cell type that demonstrates an increased susceptibility to stress and the properties of the surrounding microenvironment.^[25] We prepare a peptide-functionalized (Arg–Gly–Asp, RGD) alginate (MVG, Novamatrix) using carbodiimide chemistry.^[7] The RGD sequence offers integrin binding sites that allow the attachment

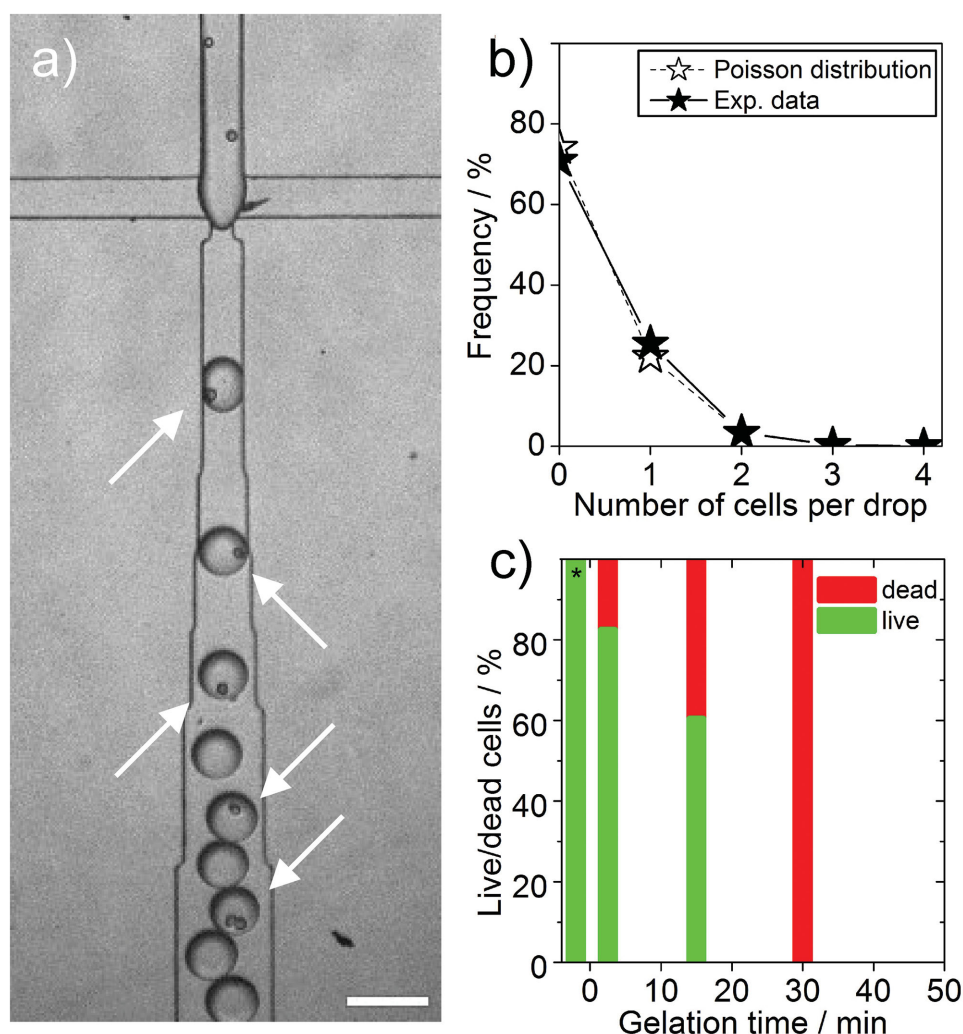


Figure 3. Microfluidic fabrication of cell-laden microbeads. a) Cells are encapsulated using a $50 \mu\text{m}$ flow-focusing device (scale bar: $100 \mu\text{m}$). Single-cell containing droplets are indicated by white arrows. b) The encapsulation process follows the Poisson distribution and results in approximately 25% of single-cell containing droplets with negligible multicell encapsulation. c) The cell viability is highly dependent on the gelation time of the microbeads. By limiting the gelation time to 2 min, a cell viability of 83% after encapsulation is achieved (* = viability of cells before encapsulation).

of the encapsulated cells to the alginate network, a necessary requirement for cellular growth of adherent cells such as MSCs.^[7,25] After dissolution of the RGD-labeled alginate (2 wt%) in cell culture medium (DMEM supplemented with 10% FBS and 1% penicillin/streptomycin (Invitrogen), the calcium–EDTA complex (50×10^{-3} M) is added and the solution is vortexed to ensure homogenous mixing. Prior to emulsification, the cells are routinely cultured, trypsinized, and resuspended in the alginate–calcium–EDTA solution. We use a cell density of 3.6×10^6 cells mL⁻¹. The cell-containing alginate–Ca–EDTA mixture is emulsified into monodisperse droplets using a flow-focusing device as shown in Figure 3a. We find that this cell density results in 25% of the droplets generated carrying single cells, while the majority of drops (70%) remain empty. The number of drops in which more than one cell is encapsulated is small, and is in good agreement with the number expected from the Poisson distribution as illustrated in Figure 3b.^[26,27] This number can be set by adjusting the cell density accordingly.^[26] Gelation of the droplets is induced by subsequent addition of acetic acid (0.05 vol%) to the oil phase. Under these conditions, we find that a crosslinking time of 2 min is sufficient to ensure complete gelation of the droplets. After crosslinking, the gels are washed to remove residual acid and EDTA and redispersed in the cell culture medium. Using a calcein–AM assay, we stain the living cells inside the microgels and find that 83% of the cells remain viable after encapsulation and crosslinking. Longer crosslinking times, i.e., extended exposure of the encapsulated cells to the acidic environment result in increased cell mortality. After 30 min of crosslinking no living cells remain as illustrated in Figure 3c. Higher concentrations of acetic acid during the crosslinking period show the same effect (data not

shown). Lower concentrations of acetic acid are not sufficient to induce complete gelation of the particles as shown in Figure S3 (Supporting Information). We incubate and culture the encapsulated MSCs under a CO₂ atmosphere at 37 °C to ensure optimal culturing conditions. The cells are clearly embedded in the microcompartments formed by the alginate hydrogels; the microgels remain intact and we observe no leakage of cells after encapsulation or while being cultured. We find that the cells keep their spherical shape when being cultured inside the microgel particle as shown in Figure 4a; this has also been reported for bulk 3D culture systems.^[25,28] Huebsch et al. were able to show that cells encapsulated in RGD-functionalized alginate interact with the surrounding matrix via α_v integrins, while maintaining their spherical shape.^[25] The cells are therefore able to adhere to the hydrogel matrix and maintain in a healthy and viable state inside the hydrogel matrix. After incubating the cells for several days, we see growth and proliferation of the cells inside the microgel particles. We observe cell division reflected by an increase in the number of cells present in the microgel matrix as is shown, for example, for cell-containing microgels that had been encapsulated for 15 days in Figure 4b. We find a high cell viability of 70% after two weeks of culture and observe only a slight decrease in the cell viability with proceeding incubation time as illustrated in Figure 4c. We believe that the cell viability can be further increased by adjustment of the hydrogel's mechanical properties and degradation behavior. The degradation behavior of alginate can be enhanced by γ -irradiation or controlled oxidation that has been shown to significantly improve the viability of encapsulated cells.^[29,30] Alternatively, composites of alginate and a degradable polymer like gelatin can be used to enhance the cell viability during

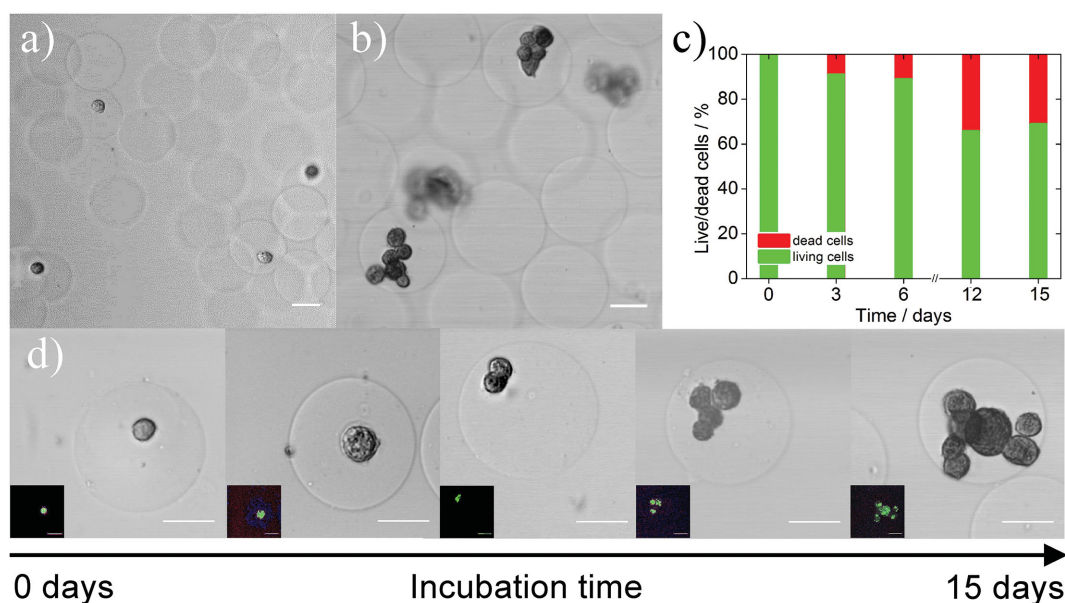


Figure 4. a) Microscopic image of alginate microgels directly after cell encapsulation and transfer into aqueous medium. In good agreement with the Poisson statistics, the majority of gels are empty and several single-cell containing gels are visible. b) After 15 days in culture, gels containing multiple cells are present. We observe no leakage of cells or disintegration of the microgel matrix during this period. c) Cell viability is determined via calcein staining. After 15 days in culture we determine a viability of 70%. d) Representative images of cell-containing alginate gels directly after encapsulation and after being cultured for 3, 6, 12, and 15 days, respectively. The cells grow and proliferate inside the generated microenvironments while maintaining their spherical morphology. The encapsulated cells are stained using a calcein assay and analyzed via a confocal laser scanning microscope to determine the cell viability (inlets). All scale bars are 25 μ m.

long-term culture.^[31,32] Nevertheless, the cellular growth and proliferation observed confirm efficient solid support as well as sufficient delivery of nutrients and oxygen to the encapsulated cells as shown in Figure 4d. This method can thus not only be used for the encapsulation of living cells but also for culturing of cells in highly controlled microgel matrices and may help to gain insights into cellular behavior in 3D environments. Additionally, the described incorporation of degradable moieties can be used to investigate cell–matrix interactions in further detail and study the self-organization of cells with proceeding degradation of the surrounding matrix.

In conclusion, we present a new method for the microfluidic fabrication of monodisperse alginate microgels with superior structural homogeneity. The use of a water-soluble calcium complex as a crosslinking precursor allows us to homogeneously distribute calcium ions within the generated alginate droplets. Subsequently, the dissociation of the complex is triggered by pH reduction resulting in the gelation of the droplets. We present the suitability of this approach for the encapsulation of living mesenchymal stem cells that are cultured inside the generated microenvironments for 15 days. During this period, we observe a stable encapsulation, cell growth, and proliferation. We believe that this method will enable a precise tuning of the mechanical properties of the microgel through control of the amount of crosslinker and the nature of the alginate chains. This will help generate reliable 3D cell culture systems for the investigation of the relation between matrix characteristics and cell behavior in 3D which is of major importance for stem cell research, wound healing, and the treatment of diseases. The small size of the microgels is attractive for applications such as injectable cell-delivery systems in regenerative medicine allowing the delivery of cells to repair damaged tissue in a minimally invasive fashion. Finally, these tailored microenvironments serve as building blocks that can be assembled into more complex structural arrangements mimicking the complexity of real biological systems such as tissues or organs. Thus, more realistic model systems are available which will result in more physiologically relevant data obtained from in vitro cultures, for example, in drug testing and development or tissue engineering applications.

Supporting Information

Supporting Information is available from the Wiley Online Library or from the author.

Acknowledgements

This work was supported by the National Institute of Health (R01 EB014703 and P01GM096971), the National Science Foundation (DMR-1310266), and the Harvard MRSEC (DMR-0820484). S.U. was supported by Deutsche Forschungsgemeinschaft (DFG). R.P. would like to thank the Fulbright Foundation for financial support (N0009552407).

Received: January 9, 2015

Revised: April 3, 2015

Published online: June 3, 2015

- [1] K. Y. Lee, D. J. Mooney, *Prog. Polym. Sci.* **2012**, *37*, 106.
- [2] W. H. Tan, S. Takeuchi, *Adv. Mater.* **2007**, *19*, 2696.
- [3] C. J. Martinez, J. W. Kim, C. Ye, I. Ortiz, A. C. Rowat, M. Marquez, D. Weitz, *Macromol. Biosci.* **2012**, *12*, 946.
- [4] S. Sugiura, T. Oda, Y. Izumida, Y. Aoyagi, M. Satake, A. Ochiai, N. Ohkohchi, M. Nakajima, *Biomaterials* **2005**, *26*, 3327.
- [5] E. Tumarkin, E. Kumacheva, *Chem. Soc. Rev.* **2009**, *38*, 2161.
- [6] H. Wang, S. C. Leeuwenburgh, Y. Li, J. A. Jansen, *Tissue Eng. Part B Rev.* **2012**, *18*, 24.
- [7] J. A. Rowley, G. Madlambayan, D. J. Mooney, *Biomaterials* **1999**, *20*, 45.
- [8] D. Velasco, E. Tumarkin, E. Kumacheva, *Small* **2012**, *8*, 1633.
- [9] J. Wan, *Polymers* **2012**, *4*, 1084.
- [10] K. S. Huang, T. H. Lai, Y. C. Lin, *Front. Biosci.* **2007**, *12*, 3061.
- [11] A. Khademhosseini, *FASEB J.* **2014**, *28*, 82.4.
- [12] S. N. Bhatia, U. J. Balis, M. L. Yarmush, M. Toner, *FASEB J.* **1999**, *13*, 1883.
- [13] H. Zhang, E. Tumarkin, R. M. A. Sullan, G. C. Walker, E. Kumacheva, *Macromol. Rapid Commun.* **2007**, *28*, 527.
- [14] B. G. Chung, K.-H. Lee, A. Khademhosseini, S.-H. Lee, *Lab Chip* **2012**, *12*, 45.
- [15] Y. Hu, Q. Wang, J. Wang, J. Zhu, H. Wang, Y. Yang, *Biomicrofluidics* **2012**, *6*, 026502.
- [16] G. Orive, R. M. Hernández, A. R. Gascón, R. Calafiore, T. M. S. Chang, P. de Vos, G. Hortelano, D. Hunkeler, I. Lacić, A. M. J. Shapiro, J. L. Pedraz, *Nat. Med.* **2003**, *9*, 104.
- [17] H. Zhang, E. Tumarkin, R. Peerani, Z. Nie, R. M. A. Sullan, G. C. Walker, E. Kumacheva, *J. Am. Chem. Soc.* **2006**, *128*, 12205.
- [18] M. Lian, C. P. Collier, M. J. Doktycz, S. T. Retterer, *Biomicrofluidics* **2012**, *6*, 044108.
- [19] C.-H. Choi, J.-H. Jung, Y. Rhee, D.-P. Kim, S.-E. Shim, C.-S. Lee, *Biomed. Microdevices* **2007**, *9*, 855.
- [20] R. O. Hynes, *Science* **2009**, *326*, 1216.
- [21] D. E. Discher, D. J. Mooney, P. W. Zandstra, *Science* **2009**, *324*, 1673.
- [22] B. Geiger, A. Bershadsky, *Cell* **2002**, *110*, 139.
- [23] C. Holtze, A. C. Rowat, J. J. Agresti, J. B. Hutchison, F. E. Angile, C. H. J. Schmitz, S. Koster, H. Duan, K. J. Humphry, R. A. Scanga, J. S. Johnson, D. Pisignano, D. A. Weitz, *Lab Chip* **2008**, *8*, 1632.
- [24] D. Poncelet, *Ann. N. Y. Acad. Sci.* **2001**, *944*, 74.
- [25] N. Huebsch, P. R. Arany, A. S. Mao, D. Shvartsman, O. A. Ali, S. A. Bencherif, R.-J. Feliciano, D. J. Mooney, *Nat. Mater.* **2010**, *9*, 518.
- [26] S. Koster, F. E. Angile, H. Duan, J. J. Agresti, A. Wintner, C. Schmitz, A. C. Rowat, C. A. Merten, D. Pisignano, A. D. Griffiths, D. A. Weitz, *Lab Chip* **2008**, *8*, 1110.
- [27] J. Clausell-Tormos, D. Lieber, J.-C. Baret, A. El-Harrak, O. J. Miller, L. Frenz, J. Blouwolff, K. J. Humphry, S. Köster, H. Duan, C. Holtze, D. A. Weitz, A. D. Griffiths, C. A. Merten, *Chem. Biol.* **2008**, *15*, 427.
- [28] D. S. Benoit, M. P. Schwartz, A. R. Durney, K. S. Anseth, *Nat. Mater.* **2008**, *7*, 816.
- [29] H. J. Kong, M. K. Smith, D. J. Mooney, *Biomaterials* **2003**, *24*, 4023.
- [30] H. J. Kong, D. Kaigler, K. Kim, D. J. Mooney, *Biomacromolecules* **2004**, *5*, 1720.
- [31] B. Sarker, D. G. Papageorgiou, R. Silva, T. Zehnder, F. G.-E. Noor, M. Bertmer, J. Kaschta, K. Chrissafis, R. Detsch, A. R. Boccacini, *J. Mater. Chem. B* **2014**, *2*, 1470.
- [32] B. Sarker, R. Singh, R. Silva, J. A. Roether, J. Kaschta, R. Detsch, D. W. Schubert, I. Cicha, A. R. Boccacini, *PLoS One* **2014**, *9*, e107952.